

18 May 2020

### Patent Update

ANO has received the report from MSL Solution Providers in London on Saturday and the results are in line with the Board's expectations confirming the underlying science in the patent application (#2020900820) jointly owned with Astivita Limited. The two Boards are looking to commercialise the first product using zinc and hinokitiol, the subject of the patent application, which the Companies intend to market in Europe through Amazon UK. The Board is unable to predict the impact to revenue from royalties and the success of Astivita's product at this very early stage until Astivita release the product, and do not expect this to have a material effect on the results in FY2020. The complete report from MSL Solutions Providers are attached along with the related research article from the Medical University of Vienna.

Authorised by:

Geoff Acton (B.Com CA)

Managing Director

**Study Title:**  
**Quantitative suspension test for evaluation of virucidal activity  
in the medical area (Phase 2 Step1)**

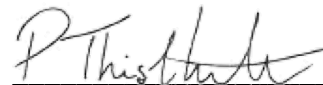
Microbiological Solutions Limited (MSL)  
Gollinrod, Walmersley, Bury, BL9 5NB, UK

Angela Davies, CEO

Customer: Antaria Pty Ltd  
Contact name: Joseph Mizkovsky  
Email: ceo@astivita.com.au  
Address:  
Report date: 15/05/2020  
PO/Quote number: Q002371



Megan Barrett  
Laboratory Manager



Peter Thistlethwaite  
Technical Projects Manager

The test results on this report refer only to the items tested as supplied by the customer. This report shall not be reproduced except in full and with written approval of Microbiological Solutions Ltd. All reports are archived for a minimum of 2 years. The sample will be retained for 1 month unless otherwise requested in writing.

**Scope**

The standard method BS EN 14476 describes a test method and the minimum requirements for virucidal activity of a chemical disinfectant and antiseptic products that form a homogenous physically stable preparation when diluted with hard water – or in the case of ready to use products that are not diluted when applied, - with water. Products can only be tested at a concentration of 80% (97% with a modified method for special cases) as some dilution is always produced by adding the test organisms and interfering substances. This European Standard applies to products that are used in the medical area in the fields of hygienic handrub, hygienic handwash, instrument disinfection by immersion, surface disinfection by wiping, spraying, flooding or other means and textile disinfection.

This European standard applies to areas and situations where disinfection is medically indicated. Such indication occurs in patient care, for example: In hospitals, in community medical facilities and in dental institutions or in clinics of schools, of kindergartens and of nursing homes, and may occur in the workplace and in the home. It may also include services such as laundries and kitchens supplying products directly for patients.

**Outline of Test Method (Obligatory Test Conditions)**

A sample of the test product is diluted in synthetic hard water in products diluted at point of use or water in the case of ready to use products is added to a test suspension of viruses in a solution of interfering substance. The mixture is maintained at one of the temperatures and contact times specified in the standard. At the end of this contact time, an aliquot is taken; the virucidal action in this portion is immediately suppressed by a validated method (dilutions of the sample in ice-cold cell maintenance medium). The dilutions are transferred into cell culture units either using monolayer or cell suspension. Infectivity tests are done either by plaque test or quantal tests. After incubation, the titres of infectivity are calculated according to Spearman and Käber or by plaque counting. Reduction of virus infectivity is calculated from differences of lg virus titres before (virus control) and after treatment with the product.

**Acceptance Criteria**

The product when tested as above shall demonstrate at least a 4 log<sub>10</sub> reduction against the test virus. The test is deemed valid where all control requirements are met.

Test information		Deviation
Name of Product	N/S	/
Batch Number & Expiry Date	N/S	
Date of Delivery	06/04/2020	
Period of Analysis	07/05/2020-14/05/2020	
Manufacturer / Supplier	Antaria Pty Ltd	
Storage Conditions	Ambient	
Appearance of the Product	Turbid liquid	
Neutralisation Method	Dilution	
Product Diluent	Distilled water	
Test Concentrations	Neat (80%), Mid-range (50%), Non active (0.1%)	
Experimental Conditions	Clean	
Interfering Substance	Clean 0.3g/l Bovine Albumin	
Test Temperature	20°C ± 1°C	
Temperature of Incubation	37°C ±1°C for 72hrs	
Identification of the Bacterial Strains:	Feline Coronavirus, Strain Munich	1
Contact Times	5 & 60 Minutes ± 10 s	
Stability and Appearance During Test	No Change Observed (Homogenous)	

**Deviations from Standard Method**


1 – The product was tested against nonstandard organism Feline coronavirus; therefore reference inactivation controls were not performed due to no acceptance criteria available.


**Test Result Summary**


The test product received has achieved a 4-log reduction against Feline coronavirus when tested under the condition stipulated in this report, with a 1-hour contact time.


*See page 2 for acceptance criteria and raw data tables below for complete test results.*


Summary

					
Conditions	Concentration	Contact time	log TCID50	log reduction	Control validation
Virus control (water)	N/A	5 minutes	7.00	N/A	Validated
Cytotoxicity (product)	Neat	N/A	2.50	N/A	Validated
Product supression control	Neat	Neat	7.04	-0.04	Validated

					
Conditions	Concentration	Contact time	log TCID50	log reduction	Control validation
Virus control (water)	N/A	1 Hour	6.75	N/A	Validated

					
Condition	Concentration	Contact time	log TCID50	Log difference	Control validation
Interference control (untreated)	N/A	N/A	7.71	N/A	N/A
Interference control (treated)	Neat	N/A	7.58	0.13	Validated

				
Condition	Concentration	Contact time	log TCID50	log reduction
Test product	Neat	5 minutes	3.75	3.25
Test product	50%	5 minutes	5.08	1.92
Test product	0.10%	5 minutes	7.08	-0.08

				
Condition	Concentration	Contact time	log TCID50	log reduction
Test product	Neat	1 Hour	2.75	4.00
Test product	50%	1 Hour	5.08	1.67
Test product	0.10%	1 Hour	6.92	-0.17

Raw data

Virus control (water)				Contact time			1 Hour	
Dilution	Counts						% CPE	p(1-p)
-2	4	4	4	4	4	4	1	0
-3	4	4	4	4	4	4	1	0
-4	4	4	4	4	4	4	1	0
-5	4	4	4	4	4	4	1	0
-6	4	4	4	4	4	4	1	0
-7	2	2	1	1	0	0	0.25	0.1875
-8	0	0	0	0	0	0	0	0
-9	0	0	0	0	0	0	0	0

Organism <i>Feline Coronavirus</i> Strain Munich	
d	1
sum px	1.25
n	8
SD50	-6.75
SE	0.16
xp	-6

Test product		Product concentration			Neat	Contact time		1 Hour	
Dilution	Counts						% CPE	p(1-p)	
-2	4	4	4	4	4	4	1	0	
-3	2	2	2	0	0	0	0.25	0.1875	
-4	0	0	0	0	0	0	0	0	
-5	0	0	0	0	0	0	0	0	
-6	0	0	0	0	0	0	0	0	
-7	0	0	0	0	0	0	0	0	
-8	0	0	0	0	0	0	0	0	
-9	0	0	0	0	0	0	0	0	

Organism <i>Feline Coronavirus</i> Strain Munich	
d	1
sum px	1.25
n	8
SD50	-2.75
SE	0.16
xp	-2

Test product		Product concentration			50%	Contact time		1 Hour	
Dilution	Counts						% CPE	p(1-p)	
-2	4	4	4	4	4	4	1	0	
-3	4	4	4	4	4	4	1	0	
-4	4	4	4	4	4	4	1	0	
-5	3	3	3	2	1	2	0.58333333	0.243056	
-6	0	0	0	0	0	0	0	0	
-7	0	0	0	0	0	0	0	0	
-8	0	0	0	0	0	0	0	0	
-9	0	0	0	0	0	0	0	0	

Organism <i>Feline Coronavirus</i> Strain Munich	
d	1
sum px	1.58
n	8
SD50	-5.08
SE	0.19
xp	-4

Test product		Product concentration			0.10%	Contact time		1 Hour	
Dilution	Counts						% CPE	p(1-p)	
-2	4	4	4	4	4	4	1	0	
-3	4	4	4	4	4	4	1	0	
-4	4	4	4	4	4	4	1	0	
-5	4	4	4	4	4	4	1	0	
-6	3	3	3	4	4	4	0.875	0.109375	
-7	3	2	1	1	2	2	0.45833333	0.248264	
-8	1	1	0	0	0	0	0.08333333	0.076389	
-9	0	0	0	0	0	0	0	0	

Organism <i>Feline Coronavirus</i> Strain Munich	
d	1
sum px	2.42
n	8
SD50	-6.92
SE	0.25
xp	-5

Raw data

Virus control (water)				Contact time			5 minutes		% CPE	p(1-p)
Dilution	Counts									
-2	4	4	4	4	4	4	4	1	0	
-3	4	4	4	4	4	4	4	1	0	
-4	4	4	4	4	4	4	4	1	0	
-5	4	4	4	4	4	4	4	1	0	
-6	4	4	4	4	4	4	4	1	0	
-7	2	2	2	2	1	1	0.41666667	0.243056		
-8	1	1	0	0	0	0	0.08333333	0.076389		
-9	0	0	0	0	0	0	0	0		

Organism <i>Feline Coronavirus</i> Strain Munich	
d	1
sum px	1.50
n	8
SD50	-7.00
SE	0.21
xp	-6

Cytotoxicity (product)				Product concentration			Neat		% CPE	p(1-p)
Dilution	Counts									
-2	4	4	4	4	4	4	4	1	0	
-3	0	0	0	0	0	0	0	0	0	
-4	0	0	0	0	0	0	0	0	0	
-5	0	0	0	0	0	0	0	0	0	
-6	0	0	0	0	0	0	0	0	0	
-7	0	0	0	0	0	0	0	0	0	
-8	0	0	0	0	0	0	0	0	0	
-9	0	0	0	0	0	0	0	0	0	

Organism <i>Feline Coronavirus</i> Strain Munich	
d	1
sum px	1.00
n	8
SD50	-2.50
SE	0.00
xp	-2

Product supression control				Product concentration			Neat		% CPE	p(1-p)
Dilution	Counts									
-2	4	4	4	4	4	4	4	1	0	
-3	4	4	4	4	4	4	4	1	0	
-4	4	4	4	4	4	4	4	1	0	
-5	4	4	4	4	4	4	4	1	0	
-6	4	4	4	4	4	4	4	1	0	
-7	2	2	2	2	2	0	0.41666667	0.243056		
-8	1	1	0	0	0	1	0.125	0.109375		
-9	0	0	0	0	0	0	0	0		

Organism <i>Feline Coronavirus</i> Strain Munich	
d	1
sum px	1.54
n	8
SD50	-7.04
SE	0.22
xp	-6

Interference control (untreated)				Product concentration			Neat		% CPE	p(1-p)
Dilution	Counts									
-1	4	4	4	4	4	4	4	1	0	
-2	4	4	4	4	4	4	4	1	0	
-3	4	4	4	4	4	4	4	1	0	
-4	4	4	4	4	4	4	4	1	0	
-5	4	4	4	4	4	4	4	1	0	
-6	4	4	4	4	4	4	4	1	0	
-7	3	3	4	4	4	4	0.91666667	0.076389		
-8	2	2	2	1	0	0	0.29166667	0.206597		
-9	0	0	0	0	0	0	0	0		
-10	0	0	0	0	0	0	0	0		

Organism <i>Feline Coronavirus</i> Strain Munich	
d	1
sum px	2.2083
n	10
SD50	-7.708
SE	0.1773
xp	-6

Raw data

Interference control (treated)		Product concentration					Neat	
Dilution	Counts						% CPE	p(1-p)
-1	4	4	4	4	4	4	1	0
-2	4	4	4	4	4	4	1	0
-3	4	4	4	4	4	4	1	0
-4	4	4	4	4	4	4	1	0
-5	4	4	4	4	4	4	1	0
-6	4	4	4	4	4	4	1	0
-7	4	4	2	2	2	2	0.66666667	0.222222
-8	1	1	2	2	3	1	0.41666667	0.243056
-9	0	0	0	0	0	0	0	0
-10	0	0	0	0	0	0	0	0

Organism <i>Feline Coronavirus</i> Strain Munich	
d	1
sum px	2.0833
n	10
SD50	-7.583
SE	0.2274
xp	-6

Test product		Product concentration					Neat		Contact time		5 minutes	
Dilution	Counts							% CPE		p(1-p)		
-2	4	4	4	4	4	4	4	1		1	0	
-3	4	4	4	4	4	4	4	1		1	0	
-4	3	3	0	0	0	0	0	0.25		0.1875		
-5	0	0	0	0	0	0	0	0		0	0	
-6	0	0	0	0	0	0	0	0		0	0	
-7	0	0	0	0	0	0	0	0		0	0	
-8	0	0	0	0	0	0	0	0		0	0	
-9	0	0	0	0	0	0	0	0		0	0	

Organism <i>Feline Coronavirus</i> Strain Munich	
d	1
sum px	1.25
n	8
SD50	-3.75
SE	0.16
xp	-3

Test product		Product concentration					50%		Contact time		5 minutes	
Dilution	Counts							% CPE		p(1-p)		
-2	4	4	4	4	4	4	4	1		1	0	
-3	4	4	4	4	4	4	4	1		1	0	
-4	4	4	4	4	4	4	4	1		1	0	
-5	3	3	3	2	1	2	0.58333333	0.243056				
-6	0	0	0	0	0	0	0	0		0	0	
-7	0	0	0	0	0	0	0	0		0	0	
-8	0	0	0	0	0	0	0	0		0	0	
-9	0	0	0	0	0	0	0	0		0	0	

Organism <i>Feline Coronavirus</i> Strain Munich	
d	1
sum px	1.58
n	8
SD50	-5.08
SE	0.19
xp	-4

Test product		Product concentration					0.10%		Contact time		5 minutes	
Dilution	Counts							% CPE		p(1-p)		
-2	4	4	4	4	4	4	4	1		1	0	
-3	4	4	4	4	4	4	4	1		1	0	
-4	4	4	4	4	4	4	4	1		1	0	
-5	4	4	4	4	4	4	4	1		1	0	
-6	4	4	4	4	4	4	4	1		1	0	
-7	3	2	1	2	2	2	0.5	0.25				
-8	1	1	0	0	0	0	0.08333333	0.076389				
-9	0	0	0	0	0	0	0	0		0	0	

Organism <i>Feline Coronavirus</i> Strain Munich	
d	1
sum px	1.58
n	8
SD50	-7.08
SE	0.22
xp	-6







# Antiviral Activity of the Zinc Ionophores Pyrithione and Hinokitiol against Picornavirus Infections<sup>∇</sup>

B. M. Krenn,<sup>1</sup> E. Gaudernak,<sup>1</sup> B. Holzer,<sup>1</sup> K. Lanke,<sup>2</sup> F. J. M. Van Kuppeveld,<sup>2</sup> and J. Seipelt<sup>1\*</sup>

Max F. Perutz Laboratories, Medical University of Vienna, Dr. Bohr-Gasse 9/3, 1030 Vienna, Austria,<sup>1</sup> and Department of Medical Microbiology, Radboud University Nijmegen Medical Centre, Nijmegen Centre for Molecular Life Sciences, 6500 HB Nijmegen, The Netherlands<sup>2</sup>

Received 22 July 2008/Accepted 6 October 2008

**We have discovered two metal ion binding compounds, pyrithione (PT) and hinokitiol (HK), that efficiently inhibit human rhinovirus, coxsackievirus, and mengovirus multiplication. Early stages of virus infection are unaffected by these compounds. However, the cleavage of the cellular eukaryotic translation initiation factor eIF4GI by the rhinoviral 2A protease was abolished in the presence of PT and HK. We further show that these compounds inhibit picornavirus replication by interfering with proper processing of the viral polyprotein. In addition, we provide evidence that these structurally unrelated compounds lead to a rapid import of extracellular zinc ions into cells. Imported Zn<sup>2+</sup> was found to be localized in punctate structures, as well as in mitochondria. The observed elevated level of zinc ions was reversible when the compounds were removed. As the antiviral activity of these compounds requires the continuous presence of the zinc ionophore PT, HK, or pyrrolidine-dithiocarbamate, the requirement for zinc ions for the antiviral activity is further substantiated. Therefore, an increase in intracellular zinc levels provides the basis for a new antipicornavirus mechanism.**

Curing virus infections harbors an enormous economic potential, and the search for new antiviral substances is of great interest for worldwide health. We have previously described the commonly used NF- $\kappa$ B inhibitor and metal ion chelator pyrrolidine-dithiocarbamate (PDTC) to significantly inhibit the replication of several picornaviruses such as human rhinovirus (HRV), poliovirus, coxsackievirus, and mengovirus (9, 22). These examples suggest that a common step in the life cycle of these picornaviruses is the target for the antiviral drug. In particular, we have demonstrated that PDTC has negative effects on picornavirus replication by influencing the processing of the viral polyprotein (21, 22).

The antiviral activity of PDTC is not restricted to the family *Picornaviridae*, since PDTC was shown to prevent the multiplication of human influenza virus, a member of the *Orthomyxoviridae* (33, 34). However, due to strong differences in the life cycle and host-cell interaction between human influenza virus and picornaviruses, it is likely that entirely different mechanisms might be relevant for the antiviral action of PDTC against these viruses.

Currently, the precise mode of the antiviral action of PDTC is unknown, although several theories have been substantiated with experimental evidence. Antioxidative properties of PDTC are postulated to be the reason for antiviral effects against influenza virus infections (33), which is not the case for human rhinovirus multiplication (9).

We have demonstrated that the antiviral effects of PDTC are metal ion dependent, and, in particular, Zn<sup>2+</sup> ions play a pivotal role. To underline the hypothesis that influx of zinc into

the cells has antiviral capacity, pyrithione (PT) and hinokitiol (HK) were examined. PT is known to be a zinc ionophore that leads to a rapid increase in intracellular zinc levels (27), and HK is a chelator of divalent metal ions (2).

We provide evidence that both PT and HK inhibit replication of picornaviruses by impairing viral polyprotein processing. The basis of the antiviral activity is dependent upon the availability of zinc ions. We show that the import of extracellular zinc ions is a key feature of the common antiviral property of these compounds.

## MATERIALS AND METHODS

**Cell, media, and reagents.** HeLa cells (strain Ohio; European Collection of Cell Cultures, Salisbury, United Kingdom) were cultured in RPMI 1640 supplemented with 10% heat-inactivated fetal calf serum, 2 mM L-glutamine, 100 U/ml penicillin, and 100  $\mu$ g/ml streptomycin (all obtained from Gibco, Invitrogen, Austria). PDTC (pyrrolidine-dithiocarbamate ammonium salt), pyrithione (2-mercaptopyridine *N*-oxide sodium salt), Zn-EDTA, Ca-EDTA, Mg-EDTA, and *N,N,N',N'*-tetrakis (2-pyridylmethyl) ethylenediamine (TPEN) were purchased from Sigma-Aldrich, Austria. HK ( $\beta$ -thujaplicin) from Calbiochem was dissolved in dimethyl sulfoxide and stored at  $-20^{\circ}\text{C}$ .

**Virus preparation and titration.** Strain HRV2 was obtained from the American Type Culture Collection and routinely grown in suspension cultures of HeLa cells (strain Ohio; Flow Laboratories, McLean, VA) as described previously (31). CVB3 (Nancy strain) was derived from transcription of the p53CVB3/T7 plasmid (36). The mengovirus strain EMCV was obtained upon transfection of in vitro-transcribed RNA from cDNA clone pM16.1 (5).

Virus titers in 50% tissue culture infectious doses (TCID<sub>50</sub>) were determined according to Reed and Muench (26). From our experience, typical interassay variation is less than  $\pm 0.5$  log TCID<sub>50</sub>/ml.

**Infection of cells.** HeLa cells were grown in six-well plates and infected at 70% confluence with HRV2 with indicated multiplicity of infection (MOI) in RPMI medium supplemented with 2% fetal calf serum, 2 mM L-glutamine, 100 U/ml penicillin, and 100  $\mu$ g/ml streptomycin. After 2 h of infection, input virus was removed, and cells were washed three times with acidic HEPES buffer and once with phosphate-buffered saline (PBS). For further incubation, infection medium was applied for the indicated amounts of times. If indicated, chemicals were present during parts or the whole period of infection. Whenever HK was used,

\* Corresponding author. Mailing address: Max F. Perutz Laboratories, Medical University of Vienna, Dr. Bohr-Gasse 9/3, 1030 Vienna, Austria. Phone: 43 1 427761610. Fax: 43 1 42779616. E-mail: joachim.seipelt@meduniwien.ac.at.

<sup>∇</sup> Published ahead of print on 15 October 2008.

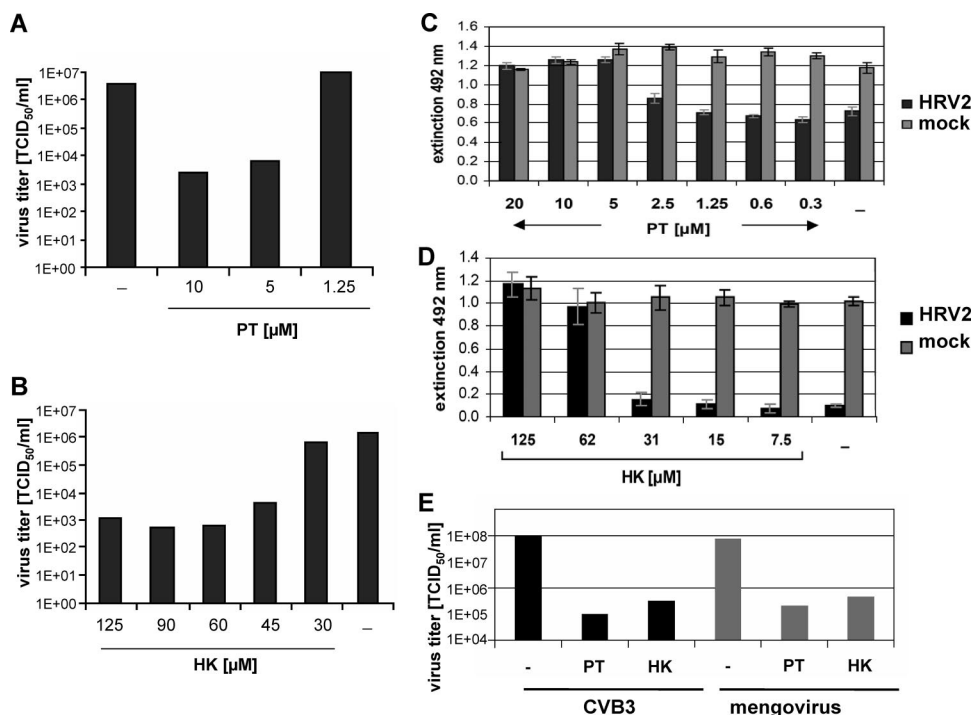


FIG. 1. PT and HK dramatically reduce picornavirus multiplication and increase cell viability. Viral titers of HRV2-infected HeLa cells (MOI = 20) in the presence or absence of indicated concentrations of PT (A) or HK plus 30 mM MgCl<sub>2</sub> (B) were determined 24 h p.i. Results for one representative experiment of three experiments are shown. HeLa cells were infected with HRV2 (MOI = 50) or mock infected, and different concentrations of PT (C) or HK-MgCl<sub>2</sub> (D) were added. At 24 h p.i., a CellTiter 96 AQ<sub>ucous</sub> nonradioactive cell proliferation assay was performed according to the manufacturer's protocol. Extinction at 492 nm reflects cell viability. The means  $\pm$  standard deviations of quintuples obtained in one representative experiment of three performed are shown. (E) HeLa cells were infected with CVB3 or mengovirus (MOI = 10) and incubated with 10  $\mu$ M PT or 75  $\mu$ M HK-30 mM MgCl<sub>2</sub>, respectively. Virus production of infected cells was determined by TCID<sub>50</sub> assay at 24 h p.i. The results for one of two representative experiments are shown. -, control.

application of 30 mM MgCl<sub>2</sub> was essential to avoid cytotoxicity. Virus production was determined in the supernatants of infected cells by TCID<sub>50</sub> determination.

Confluent monolayers of HeLa cells were infected with CVB3 or mengovirus for 30 min. Cells were then washed twice with PBS and cultured in medium at 37°C in the presence or absence of indicated chemicals. At indicated time points, the cells were disrupted by three cycles of freezing and thawing, and virus titers were determined by end point titration.

**Cell viability assay.** HeLa cells were infected with HRV2 (MOI = 50) or mock infected in the presence or absence of different concentrations of PT or HK-MgCl<sub>2</sub>. At 24 h postinfection (p.i.), a CellTiter 96 AQ<sub>ucous</sub> nonradioactive cell proliferation assay (Promega, WI) was performed according to the manufacturer's protocol. Extinction at 492 nm reflecting cell viability was measured in a Labsystems Multiscan RC plate reader.

**Western blot analysis.** HeLa cells were infected with HRV2 as described for virus infection. At 0, 2, 4, 6, 8, and 24 h p.i., the medium was removed, and the cells were lysed by the addition of protein sample buffer. Protein extracts were subjected to sodium dodecyl sulfate-polyacrylamide gel electrophoresis (SDS-PAGE), electroblotted onto polyvinylidene difluoride membranes, and analyzed using a rabbit polyclonal antibody against eIF4G1 (37), as described previously (9).

**Pulse-labeling and immunoprecipitation.** HeLa cells were preincubated with 10  $\mu$ M PT or 125  $\mu$ M HK-30 mM MgCl<sub>2</sub> for 30 min and infected with HRV2 (MOI = 50) in the presence of the substances. At 6 h p.i., newly synthesized proteins were labeled with [<sup>35</sup>S]Met/Cys (Hartmann Analytic, Germany) for 1 hour. At 7, 8, and 9 h p.i., VP2 or VP2-comprising precursor proteins were isolated by immunoprecipitation using the monoclonal VP2-specific 8F5 antibodies (30) and analyzed by SDS-PAGE and autoradiography as described previously (21).

HeLa cells infected with CVB3 (MOI = 50) were incubated with 125  $\mu$ M PDTC, 75  $\mu$ M HK-30 mM MgCl<sub>2</sub>, or 10  $\mu$ M PT in the presence or absence of 10  $\mu$ M TPEN. Five hours p.i., cells were starved half an hour prior to 1 h of labeling with [<sup>35</sup>S]Met/Cys. After labeling, cells were lysed, and cellular extracts

were subjected to immunoprecipitation using either antibodies specific for 3D or 3C (kindly provided by C. Cameron, Pennsylvania State University) as described previously (22). Then, the protein pattern was analyzed by SDS-PAGE and autoradiography.

**Radioactive zinc uptake studies.** HeLa cells in serum-free culture medium (zinc concentration of 0.6  $\mu$ M as measured by atomic absorption analysis) were incubated with 5  $\mu$ M <sup>65</sup>Zn<sup>2+</sup> (0.82 mCi/mg Zn<sup>2+</sup>; Hartmann Analytic, Germany) in the presence of indicated concentrations of PDTC, PT, or HK-MgCl<sub>2</sub>. At the indicated time points, the cells were harvested by filtration on GF/C glass fiber filters (Whatman, Maidstone, United Kingdom). To remove extracellular <sup>65</sup>Zn<sup>2+</sup>, filters were washed with a buffer containing EDTA (15 mM HEPES, 100 mM glucose, 150 mM KCl, 1 mM EDTA [pH 7]), and the amount of intracellular <sup>65</sup>Zn<sup>2+</sup> was determined in a Packard Cobra II  $\gamma$ -counter.

**Fluorescence microscopy.** HeLa cells grown in  $\mu$ -slide VI slides (Ibidi, Germany) were loaded with 5  $\mu$ M FluoZin-3 acetoxymethyl ester (Invitrogen) or 1  $\mu$ M RhodZin-3 acetoxymethyl ester (Invitrogen) in PBS for 15 min at 37°C. Subsequently, cells were incubated for 1 h in growth medium to allow de-esterification. Then, PDTC, PT, or HK was added to the medium for the indicated incubation times. In some experiments, chemicals were removed after 30 min, and fresh medium was applied for 1 h. Fluorescence was monitored in a live-cell microscope system (Olympus cellIR) using fluorescein isothiocyanate settings for FluoZin-3 and Cy3 settings for RhodZin-3. A Hamamatsu Photonics Orca-ER camera was used.

## RESULTS AND DISCUSSION

**PT and HK inhibit picornavirus multiplication and increase cell viability of infected cells.** We have previously discovered that the drug PDTC substantially interferes with the multiplication of several picornaviruses (9, 22). These antiviral

effects of PDTC are dependent on metal ions, in particular zinc ions. To further substantiate the hypothesis that zinc ions play a major role in virus inhibition, two structurally different metal ion binding compounds, PT (4, 12, 17, 35) and HK (2, 23, 32), were analyzed regarding their effects on HRV production (Fig. 1). HeLa cells were infected with HRV serotype 2 with an MOI of 20 in the presence or absence of PT or HK. At 24 h p.i., supernatants were collected, and virus titers were determined. The presence of 5  $\mu$ M and 10  $\mu$ M PT decreased viral titers by around 3 orders of magnitude (Fig. 1A). Likewise, HK significantly diminished viral multiplication in a dose-dependent manner (Fig. 1B). Similar results were obtained using a different HRV serotype (HRV14) or an alveolar carcinoma cell line (A549) (data not shown).

To quantify cell viability a colorimetric viability assay was performed. HeLa cells infected with HRV2 showed a significant loss of viability 24 h p.i. (Fig. 1C and D). In contrast, PT (Fig. 1C) and HK (Fig. 1D) retained viability to normal levels at concentrations between 5  $\mu$ M and 20  $\mu$ M PT and 62  $\mu$ M and 125  $\mu$ M HK, respectively. Based on additional experiments, 50% inhibitory concentrations of 3  $\mu$ M for PT and 42  $\mu$ M for HK were determined. Importantly, no cytotoxicity of PT and HK was found in mock-infected HeLa cells (Fig. 1C and D, gray bars) and A549 cells (data not shown) under these conditions. The absence of cytotoxicity is in contrast to reports about proapoptotic activities of PT and HK in other cell lines such as HL-60 cells (15, 19, 20).

It is of great interest to investigate whether PT and HK act specifically for HRV or whether these drugs target a common step in the picornavirus life cycle. Thus, the role of PT and HK during infection with coxsackievirus strain B3 (CVB3) and the mengovirus strain EMCV (which will hereafter be referred to as mengovirus) was examined (Fig. 1E). In a single-round infection experiment with CVB3 or mengovirus, viral titers of around  $10^8$  TCID<sub>50</sub>/ml were obtained. In the presence of PT or HK, the titers were significantly reduced by around 3 and 2 orders of magnitude, respectively. These data are in agreement with the antiviral activities of PDTC against these viruses that were reported previously (22).

**PT and HK abolish eIF4GI cleavage and affect viral polyprotein processing.** Different steps of the HRV infection in the presence of PT or HK were studied to analyze whether PT and HK act mechanistically similar to PDTC. Early events in the viral life cycle, such as virus entry and uncoating, were not affected by PT and HK (data not shown). A hallmark of rhinovirus infection is the cleavage of the eukaryotic translation initiation factors eIF4GI and eIF4GII by the viral 2A<sup>pro</sup> (7, 11), leading to the shutoff of host-cell protein synthesis (8). To test whether PT and HK affect eIF4GI cleavage, protein extracts of HRV2-infected cells were analyzed by Western blotting (Fig. 2A). In the absence of PT or HK, around 50% cleavage of eIF4GI was obtained at 4 h p.i. At 6 h and 8 h p.i., eIF4GI was nearly completely processed into its typical cleavage products. In the presence of PT or HK, no significant amounts of eIF4GI cleavage products were found within 24 h of infection. This is in agreement with data obtained with PDTC (9).

As PDTC shows a clear inhibition of viral polyprotein processing (21), P1 processing was also examined in the

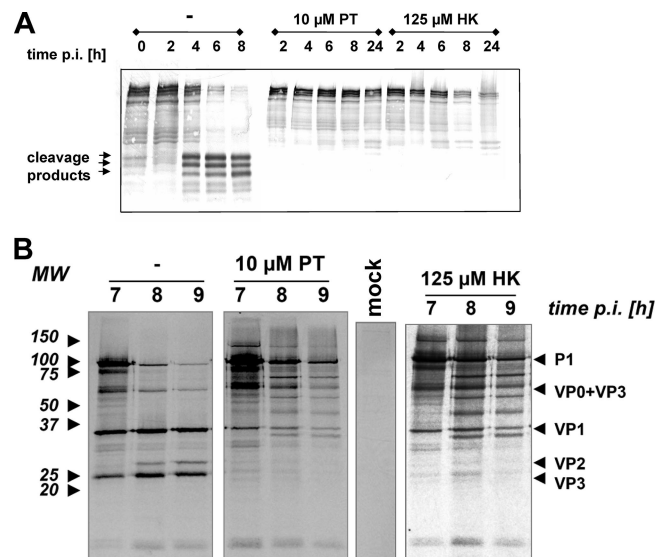


FIG. 2. PT and HK abolish HRV2-triggered eIF4GI cleavage and affect viral polyprotein processing. (A) HRV2-infected HeLa cells (MOI = 20) were either mock treated or treated with 10  $\mu$ M PT or 125  $\mu$ M HK-30 mM MgCl<sub>2</sub>. After the indicated time points, protein extracts were collected and analyzed by Western blotting using an antibody specific for eIF4GI and its cleavage products. (B) HeLa cells were preincubated with 10  $\mu$ M PT or 125  $\mu$ M HK-30 mM MgCl<sub>2</sub> for 30 min and infected with HRV2 (MOI = 50) in the presence of the substances. At 6 h p.i., newly synthesized proteins were labeled with [<sup>32</sup>S]Met/Cys for 1 hour. At the indicated time points, VP2 or VP2-containing precursor proteins were isolated by immunoprecipitation and analyzed by SDS-PAGE and autoradiography. Immunoprecipitation of mock-infected labeled cells did not show any signal. MW, molecular weight in thousands.

presence of PT or HK (Fig. 2B) by a pulse-chase labeling experiment, followed by immunoprecipitation with a VP2-specific antibody, 8F5, which pulls down VP2, VP2-containing precursors, and viral proteins bound to VP2 (30). Labeling of viral proteins started at 6 h p.i. for 60 min, and subsequently, cell lysates were prepared every hour. In untreated cells, the processing of the P1 precursor protein was clearly visible between 7 h and 9 h p.i. as a reduction of the amount of the corresponding polyprotein band. At the same time, smaller bands comprising VP2 and VP3 appeared. In the presence of either PT or HK, the processing of the P1 protein was blocked, and no mature VP2 or VP3 products could be detected. Moreover, various intermediate processing products were obtained in the presence of PT or HK, giving an identical picture to the processing defects observed using PDTC (21).

To specifically monitor the activity of 3CD<sup>pro</sup>, which is responsible for the processing of the P1 region and which autocleaves itself into 3C<sup>pro</sup> and 3D<sup>pol</sup>, the polyprotein-processing pattern of coxsackievirus infection in the presence of PDTC, PT, and HK was investigated (Fig. 3). CVB3-infected HeLa cells incubated with PDTC, HK, or PT were starved half an hour prior to 1 h of labeling at 5.5 h p.i. Subsequently, immunoprecipitation experiments using polyclonal antibodies raised against CVB3 3C<sup>pro</sup> and 3D<sup>pol</sup> were performed and analyzed as described above. PDTC, PT, and HK abolished coxsackievirus polyprotein processing into the



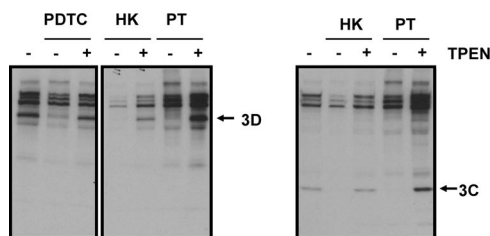


FIG. 3. PT and HK abrogate 3D and 3C processing of CVB3. HeLa cells infected with coxsackievirus B3 (MOI = 50) were incubated with 125  $\mu$ M PDTC, 75  $\mu$ M HK-30 mM  $MgCl_2$ , or 10  $\mu$ M PT in the presence or absence of 10  $\mu$ M TPEN. At 5 h p.i., cells were starved half an hour prior to 1 h of labeling with [ $^{35}S$ ]Met/Cys. Harvested cell lysates were subjected to immunoprecipitation using either antibodies specific for 3D (left panel) or 3C (right panel) and then analyzed by SDS-PAGE and autoradiography. Results for a representative experiment are shown. -, TPEN absent; +, TPEN present.

mature viral proteins 3D and 3C in a similar manner indicating a common antiviral mechanism of all three compounds. The presence of 10  $\mu$ M of the strong metal ion chelator TPEN restored viral polyprotein processing, suggesting that the observed inhibition is based on the availability of metal ions.

These data indicate that polyprotein processing of picornaviruses is a sensitive step for treatment with zinc ionophores. We have evidence that viruses such as respiratory syncytial virus (belonging to the family of *Paramyxoviridae*) which do not depend on polyprotein processing during their life cycle are not inhibited by PDTC treatment (data not shown). An unspecific adverse effect of PDTC on general

cellular functions that lead to virus inhibition is therefore unlikely.

**EDTA abolishes the antipicornavirus effects of PT and HK.** We and others have shown that treatment with PDTC or PT leads to a rapid elevation of the concentration of free cytoplasmic  $Zn^{2+}$  ions (6, 22, 16–18). The importance of metal ions was further substantiated by experiments using EDTA as a general extracellular metal ion chelator (Fig. 4). In the presence of 10  $\mu$ M EDTA, the antiviral properties of PT and HK against HRV2 (Fig. 4A), CVB3 (Fig. 4B), and mengovirus (Fig. 4C) are lost, indicating the involvement of metal ions. By using  $Zn^{2+}$ -,  $Ca^{2+}$ -, or  $Mg^{2+}$ -saturated EDTA (25), we demonstrate that only Zn-EDTA retains the antiviral property of PT or HK. This indicates that the availability of  $Zn^{2+}$  ions is a prerequisite for the antiviral activity of these compounds. None of the EDTA-metal ion complexes alone had any antiviral effect at the concentrations tested.

**PDTC, PT, and HK treatments cause a rapid and efficient influx of  $^{65}Zn^{2+}$  into cells.** It is unclear whether PDTC, PT, and HK mobilize zinc ions localized in intracellular storage vesicles or allow extracellular ions to enter the cytoplasm. To directly monitor import of extracellular zinc ions into HeLa cells, we employed radioactive  $^{65}Zn^{2+}$  to determine the effects of PT, HK, and PDTC on zinc import (Fig. 5A). HeLa cells were incubated for different time periods with 5  $\mu$ M  $^{65}Zn^{2+}$  and PDTC, PT, or HK and then harvested by filtration on GF/C glass fiber filters. The amount of intracellular  $^{65}Zn^{2+}$  was measured by  $\gamma$ -counting of the filter membranes. In the presence of  $^{65}Zn^{2+}$  alone, no significant increase in radioac-

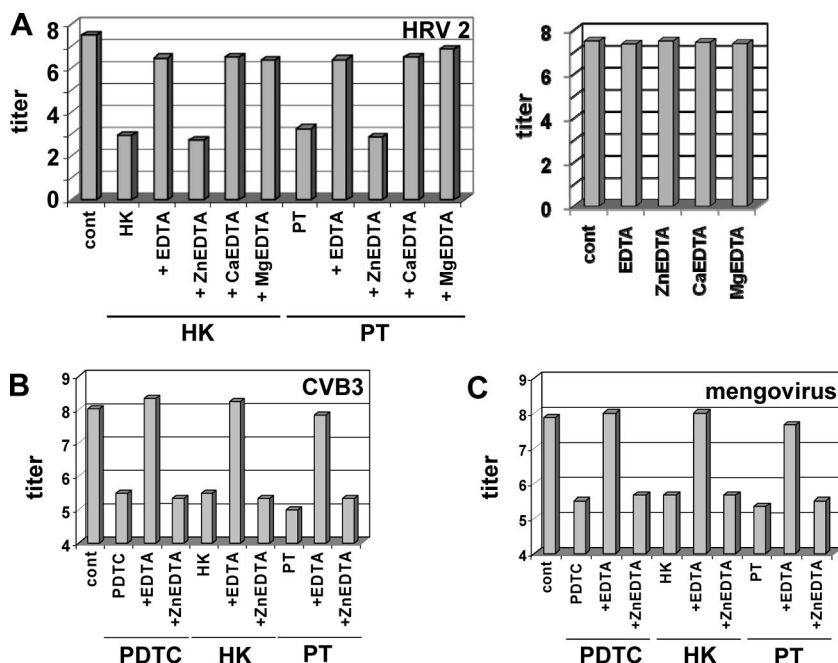


FIG. 4. Zinc ions are responsible for the antiviral property of PT and HK. HeLa cells were infected with HRV2 (MOI = 20) (A), CVB3 (MOI = 10) (B), or mengovirus (MOI = 10) (C) and incubated with 10  $\mu$ M EDTA or 10  $\mu$ M of Zn-EDTA, Ca-EDTA, and Mg-EDTA, respectively. If indicated, 10  $\mu$ M PT (A, B, and C), 125  $\mu$ M HK-30 mM  $MgCl_2$  (A), or 75  $\mu$ M HK- $MgCl_2$  (B and C) was added at the time of infection. The virus titers in the supernatants of the infected cells were determined by a TCID<sub>50</sub> assay at 24 h p.i. and shown as log TCID<sub>50</sub>/ml. Viral infection without addition of compounds is labeled as “cont.” The results for one representative experiment of three are shown.

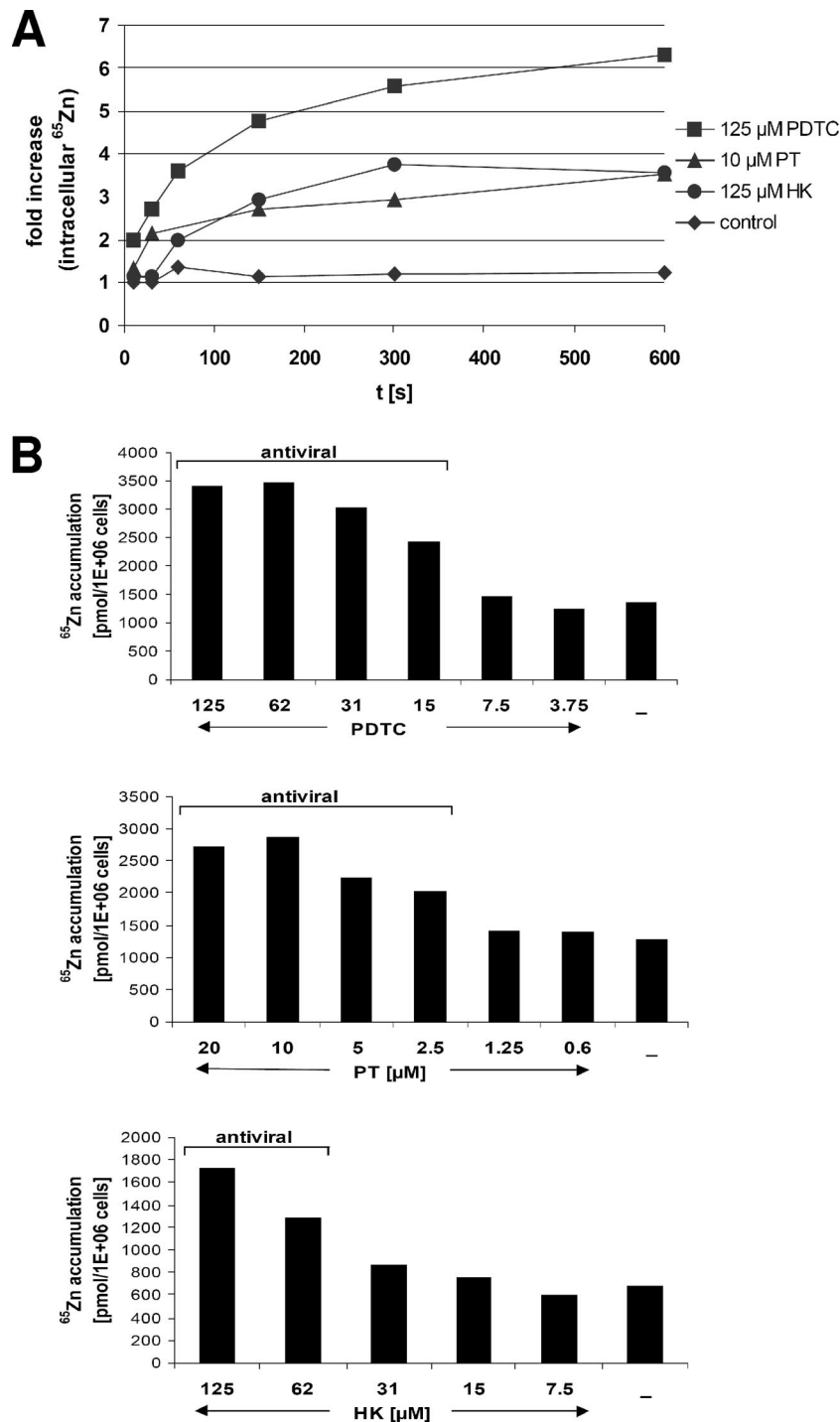


FIG. 5. PDTC, PT, and HK cause import of extracellular  $^{65}\text{Zn}^{2+}$  levels in a dose-dependent manner. (A) HeLa cells in serum-free culture medium were incubated with  $5 \mu\text{M}$   $^{65}\text{Zn}^{2+}$  and  $125 \mu\text{M}$  PDTC,  $10 \mu\text{M}$  PT, or  $125 \mu\text{M}$  HK- $30 \text{ mM}$   $\text{MgCl}_2$ . At the indicated time points, the cells were harvested and washed with a buffer containing EDTA, and the amount of intracellular  $^{65}\text{Zn}^{2+}$  was determined in a Packard Cobra II  $\gamma$ -counter. Statistical variations between different samples are determined to be a maximal  $\pm 10\%$  (data not shown). The results for one of three experiments are shown. (B) HeLa cells in serum-free culture medium were incubated with  $5 \mu\text{M}$   $^{65}\text{Zn}^{2+}$  and various concentrations of PDTC (top panel), PT (middle panel), or HK- $\text{MgCl}_2$  (lower panel) for 15 min. Then, the cells were collected and washed, and the amount of intracellular  $^{65}\text{Zn}^{2+}$  was determined as described above. The results for one of five experiments are shown.

tivity of the collected cells was measured, whereas the presence of either PT or HK facilitated a threefold increase of intracellular  $^{65}\text{Zn}^{2+}$  within a few minutes. PDTC elevated the intracellular  $^{65}\text{Zn}^{2+}$  level sixfold. These results demonstrate that all

three substances facilitate import of extracellular zinc ions via a rapid uptake mechanism.

As shown in Fig. 5B, this zinc uptake is dose dependent. The presence of more than  $15 \mu\text{M}$  PDTC,  $2.5 \mu\text{M}$  PT, or  $62 \mu\text{M}$  HK

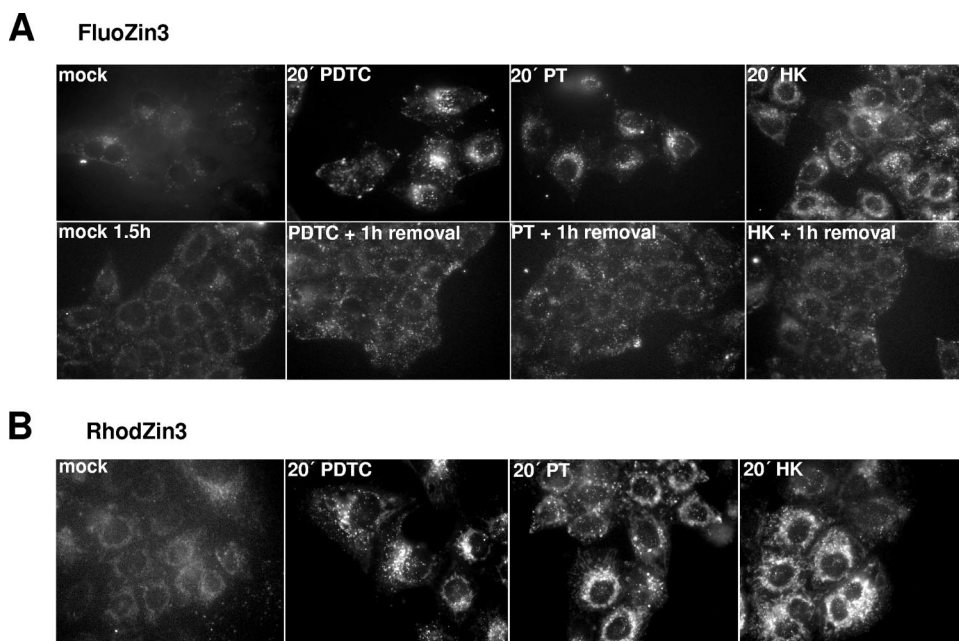


FIG. 6. Zinc ionophores influence the labile  $Zn^{2+}$  pool. HeLa cells were loaded with 5  $\mu$ M FluoZin-3 (A) or 1  $\mu$ M RhodZin-3 (B) in PBS for 15 min at 37°C. After extensive washing and 1 h of de-esterification in medium, zinc uptake was induced by treatment with 125  $\mu$ M PDTC, 10  $\mu$ M PT, and 125  $\mu$ M HK-30 mM  $MgCl_2$  in growth medium. If indicated, after 30 min of chemical treatment, ionophores were removed for 1 hour (PDTC + 1 h removal, PT + 1 h removal, HK + 1 h removal). Pictures were taken at the indicated time points by live fluorescence microscopy with 60 $\times$  optics. Examples of images of three independent experiments were chosen.

caused significant  $^{65}Zn^{2+}$  uptake after 15 min. It is noteworthy that this concentration range was found to be antiviral (Fig. 1) (9), suggesting that the influx of zinc ions is essential for mediating the common antiviral property of these compounds.

**Intracellular localization of zinc ions imported via PT, HK, and PDTC.** To directly visualize the ability of PDTC, PT, and HK to increase the intracellular pool of labile  $Zn^{2+}$ , specific zinc indicators were used (Fig. 6). FluoZin-3 is a  $Zn^{2+}$ -sensitive and -specific fluorescent probe that has no specific cellular localization (14). In cells loaded with FluoZin-3, intracellular fluorescence was minimal (Fig. 6A, top panel) due to a very low level of free zinc ions (24). After induction with 10  $\mu$ M PT, 125  $\mu$ M PDTC, or 125  $\mu$ M HK, a rapid and significant increase in fluorescence was found reflecting an elevation of the intracellular labile “chelatable” zinc level. Noteworthy, these experiments were carried out in normal growth medium and apparently the  $Zn^{2+}$  concentration present in the medium is sufficient to lead to ionophore-mediated zinc ion transport.

The observed punctate pattern of FluoZin-3 fluorescence is in agreement with recent data from rainbow trout cells incubated with high levels of extracellular zinc (24). In a large variety of mammalian cell types, vesicular storage sites for zinc which have been designated “zincosomes” can be detected (1). Zincosomes play a role in detoxifying excess zinc and are suggested to colocalize with endosomal compartments and lysosomes (13).

The uptake of zinc ions is reversible. When the zinc ionophores PDTC, PT, and HK were removed, the fluorescence declined close to background within 1 h (Fig. 6A, bottom panel).

To specifically monitor the free mitochondrial zinc pool, RhodZin-3 was used (28). HeLa cells loaded with RhodZin-3 exhibited a very weak fluorescence, indicating low levels of

labile  $Zn^{2+}$  inside the mitochondrial compartment (Fig. 6B). In contrast, upon 20 min of treatment with PDTC, PT, or HK, the signal of RhodZin-3 fluorescence was strongly enhanced. This mitochondrial localized signal was found to be constant over at least 80 min of PT incubation (data not shown). The role of a labile  $Zn^{2+}$  fraction in mitochondria during viral infection is currently unclear and has to be the subject of further studies.

**Concluding remarks.** Conclusively, all three antiviral substances are potent zinc ionophores increasing the intracellular pool of labile zinc. This strong elevation is constant as long as the zinc ionophores are present but is reversible after removal of PDTC, PT, or HK.

The reversibility of the elevation of free-zinc concentrations is in agreement with data that we had obtained when virus multiplication was monitored in a setup when PT, HK, and PDTC were present for short intervals only. In contrast to the significant viral titer reduction evoked by permanently present PDTC, PT, or HK, a short (1 h) pulse of zinc ionophore treatment between 2 h and 5 h p.i. was not sufficient to significantly reduce viral titers (data not shown). These data indicate that a prolonged presence of ionophores during viral replication is needed to exert antiviral effects. In previous data, we have shown that a clear reduction of virus titer was obtained when PDTC treatment started up to 4 h after infection, continuing to 24 h (9).

In conclusion, we have identified a set of three antiviral compounds against HRV, coxsackievirus, and mengovirus infections, which differ in their chemical structures but appear to use import of zinc ions as a common trigger for exerting their antiviral effect. It was reported that PDTC reduces coxsackie-



virus B3 replication through inhibition of the ubiquitin-proteasome pathway (29). We tested the proteasome inhibitor MG-132 at nontoxic concentrations for antiviral properties against HRV2 and HRV14. However, functional MG-132 concentrations that cause a massive accumulation of ubiquitinated proteins within 8 h of incubation were not antiviral (data not shown). Thus, proteasomal inhibition is not likely to be the major cause of the antiviral activity of PDTC, PT, or HK.

Importantly, PDTC, PT, and HK lead to efficient import of zinc ions that are naturally present in the cell culture medium. Uptake of  $Zn^{2+}$  into cells interferes with the viral life cycle. Already in 1974, Butterworth and colleagues have shown that adding high concentrations of zinc ions to cells impairs picornavirus polyprotein processing (3); however, the mechanistic basis still remains incompletely understood. On the one hand, viral proteases might be affected in their functions directly; on the other hand, zinc ions could contribute to folding problems of the viral polyprotein that lead to inseparable precursors. Folding inhibition was recently suggested as a target for antiviral strategies (10).

Several attempts have been employed to create mutants resistant against PDTC during human rhinovirus or influenza virus infections. However, no resistant viruses were obtained, hinting at a cellular mechanism of action which is expected to be similar for HK and PT. On account of these findings, PDTC, PT, and HK may provide an interesting basis for the development of new classes of antipicornaviral therapeutics.

#### ACKNOWLEDGMENTS

This work was supported by grant LS05-039 of the Vienna Science and Technology Fund to J.S. and by grant NWO-VIDI-6 917.46.305 of The Netherlands Organization for Scientific Research and the M.W. Beijerinck Virology Fund from the Royal Netherlands Academy of Sciences to F.J.M.V.K.

We thank C. Cameron (Pennsylvania State University) for the kind gift of antibodies, Andrea Trienoll for technical help, and Hans Goldenberg for helpful discussions.

#### REFERENCES

- Beyersmann, D., and H. Haase. 2001. Functions of zinc in signaling, proliferation and differentiation of mammalian cells. *Biometals* **14**:331–341.
- Bryant, F., and B. T. Overell. 1953. Quantitative chromatographic analysis of organic acids in plant tissue extracts. *Biochim. Biophys. Acta* **10**:471–476.
- Butterworth, B. E., and B. D. Korant. 1974. Characterization of the large picornaviral polypeptides produced in the presence of zinc ion. *J. Virol.* **14**:282–291.
- Crutchfield, C. E., III, E. J. Lewis, and B. D. Zelickson. 1997. The highly effective use of topical zinc pyrithione in the treatment of psoriasis: a case report. *Dermatol. Online* **3**:3.
- Duke, G. M., and A. C. Palmenberg. 1989. Cloning and synthesis of infectious coronavirus RNAs containing short, discrete poly(C) tracts. *J. Virol.* **63**:1822–1826.
- Erl, W., C. Weber, and G. K. Hansson. 2000. Pyrrolidine dithiocarbamate-induced apoptosis depends on cell type, density, and the presence of  $Cu(2+)$  and  $Zn(2+)$ . *Am. J. Physiol. Cell Physiol.* **278**:C1116–C1125.
- Etchison, D., and S. Fout. 1985. Human rhinovirus 14 infection of HeLa cells results in the proteolytic cleavage of the p220 cap-binding complex subunit and inactivates globin mRNA translation in vitro. *J. Virol.* **54**:634–638.
- Etchison, D., S. C. Milburn, I. Ederly, N. Sonenberg, and J. W. Hershey. 1982. Inhibition of HeLa cell protein synthesis following poliovirus infection correlates with the proteolysis of a 220,000-dalton polypeptide associated with eucaryotic initiation factor 3 and a cap binding protein complex. *J. Biol. Chem.* **257**:14806–14810.
- Gaudernak, E., J. Seipelt, A. Triendl, A. Grassauer, and E. Kuechler. 2002. Antiviral effects of pyrrolidine dithiocarbamate on human rhinoviruses. *J. Virol.* **76**:6004–6015.
- Geller, R., M. Vignuzzi, R. Andino, and J. Frydman. 2007. Evolutionary constraints on chaperone-mediated folding provide an antiviral approach refractory to development of drug resistance. *Genes Dev.* **21**:195–205.
- Gradi, A., H. Imataka, Y. V. Svitkin, E. Rom, B. Raught, S. Morino, and N. Sonenberg. 1998. A novel functional human eukaryotic translation initiation factor 4G. *Mol. Cell. Biol.* **18**:334–342.
- Guthery, E., L. A. Seal, and E. L. Anderson. 2005. Zinc pyrithione in alcohol-based products for skin antiseptics: persistence of antimicrobial effects. *Am. J. Infect. Control* **33**:15–22.
- Haase, H., and D. Beyersmann. 2002. Intracellular zinc distribution and transport in C6 rat glioma cells. *Biochem. Biophys. Res. Commun.* **296**:923–928.
- Haase, H., and W. Maret. 2003. Intracellular zinc fluctuations modulate protein tyrosine phosphatase activity in insulin/insulin-like growth factor-1 signaling. *Exp. Cell Res.* **291**:289–298.
- Inamori, Y., H. Tsujibo, H. Ohishi, F. Ishii, M. Mizugaki, H. Aso, and N. Ishida. 1993. Cytotoxic effect of hinokitol and tropolone on the growth of mammalian cells and on blastogenesis of mouse splenic T cells. *Biol. Pharm. Bull.* **16**:521–523.
- Kim, C. H., J. H. Kim, C. Y. Hsu, and Y. S. Ahn. 1999. Zinc is required in pyrrolidine dithiocarbamate inhibition of NF-kappaB activation. *FEBS Lett.* **449**:28–32.
- Kim, C. H., J. H. Kim, S. J. Moon, K. C. Chung, C. Y. Hsu, J. T. Seo, and Y. S. Ahn. 1999. Pyrithione, a zinc ionophore, inhibits NF-kappaB activation. *Biochem. Biophys. Res. Commun.* **259**:505–509.
- Kim, C. H., J. H. Kim, J. Xu, C. Y. Hsu, and Y. S. Ahn. 1999. Pyrrolidine dithiocarbamate induces bovine cerebral endothelial cell death by increasing the intracellular zinc level. *J. Neurochem.* **72**:1586–1592.
- Kondoh, M., E. Tasaki, S. Araragi, M. Takiguchi, M. Higashimoto, Y. Watanabe, and M. Sato. 2002. Requirement of caspase and p38MAPK activation in zinc-induced apoptosis in human leukemia HL-60 cells. *Eur. J. Biochem.* **269**:6204–6211.
- Kondoh, M., E. Tasaki, M. Takiguchi, M. Higashimoto, Y. Watanabe, and M. Sato. 2005. Activation of caspase-3 in HL-60 cells treated with pyrithione and zinc. *Biol. Pharm. Bull.* **28**:757–759.
- Krenn, B. M., B. Holzer, E. Gaudernak, A. Triendl, F. J. van Kuppeveld, and J. Seipelt. 2005. Inhibition of polyprotein processing and RNA replication of human rhinovirus by pyrrolidine dithiocarbamate involves metal ions. *J. Virol.* **79**:13892–13899.
- Lanke, K., B. M. Krenn, W. J. Melchers, J. Seipelt, and F. J. van Kuppeveld. 2007. PDTC inhibits picornavirus polyprotein processing and RNA replication by transporting zinc ions into cells. *J. Gen. Virol.* **88**:1206–1217.
- Miyamoto, D., Y. Kusagaya, N. Endo, A. Sometani, S. Takeo, T. Suzuki, Y. Arima, K. Nakajima, and Y. Suzuki. 1998. Thujaplicin-copper chelates inhibit replication of human influenza viruses. *Antiviral Res.* **39**:89–100.
- Muyllé, F. A., D. Adriaensens, W. De Coen, J. P. Timmermans, and R. Blust. 2006. Tracing of labile zinc in live fish hepatocytes using FluoZin-3. *Biometals* **19**:437–450.
- Perrin, D. D. 1979. Stability constants of metal-ion complexes: organic ligands. Pergamon, Oxford, United Kingdom.
- Reed, L. J., and H. Muench. 1938. A simple method of estimating fifty per cent endpoints. *Am. J. Hyg.* **27**:493–497.
- Sensi, S. L., L. M. Canzoniero, S. P. Yu, H. S. Ying, J. Y. Koh, G. A. Kerchner, and D. W. Choi. 1997. Measurement of intracellular free zinc in living cortical neurons: routes of entry. *J. Neurosci.* **17**:9554–9564.
- Sensi, S. L., D. Ton-That, J. H. Weiss, A. Rothe, and K. R. Gee. 2003. A new mitochondrial fluorescent zinc sensor. *Cell Calcium* **34**:281–284.
- Si, X., B. M. McManus, J. Zhang, J. Yuan, C. Cheung, M. Esfandiarei, A. Suarez, A. Morgan, and H. Luo. 2005. Pyrrolidine dithiocarbamate reduces coxsackievirus B3 replication through inhibition of the ubiquitin-proteasome pathway. *J. Virol.* **79**:8014–8023.
- Skern, T., C. Neubauer, L. Frasel, P. Grundler, W. Sommergruber, M. Zorn, E. Kuechler, and D. Blaas. 1987. A neutralizing epitope on human rhinovirus type 2 includes amino acid residues between 153 and 164 of virus capsid protein VP2. *J. Gen. Virol.* **68**:315–323.
- Skern, T., W. Sommergruber, D. Blaas, C. Pieler, and E. Kuechler. 1984. Relationship of human rhinovirus strain 2 and poliovirus as indicated by comparison of the polymerase gene regions. *Virology* **136**:125–132.
- Trust, T. J., and R. W. Coombs. 1973. Antibacterial activity of beta-thujaplicin. *Can. J. Microbiol.* **19**:1341–1346.
- Uchide, N., and K. Ohyama. 2003. Antiviral function of pyrrolidine dithiocarbamate against influenza virus: the inhibition of viral gene replication and transcription. *J. Antimicrob. Chemother.* **52**:8–10.
- Uchide, N., K. Ohyama, T. Bessho, B. Yuan, and T. Yamakawa. 2002. Effect of antioxidants on apoptosis induced by influenza virus infection: inhibition of viral gene replication and transcription with pyrrolidine dithiocarbamate. *Antiviral Res.* **56**:207–217.
- Warner, R. R., J. R. Schwartz, Y. Boissy, and T. L. Dawson, Jr. 2001. Dandruff has an altered stratum corneum ultrastructure that is improved with zinc pyrithione shampoo. *J. Am. Acad. Dermatol.* **45**:897–903.
- Wessels, E., D. Duijsings, R. A. Notebaart, W. J. Melchers, and F. J. van Kuppeveld. 2005. A proline-rich region in the coxsackievirus 3A protein is required for the protein to inhibit endoplasmic reticulum-to-Golgi transport. *J. Virol.* **79**:5163–5173.
- Yan, R., W. Rychlik, D. Etchison, and R. E. Rhoads. 1992. Amino acid sequence of the human protein synthesis initiation factor eIF-4 gamma. *J. Biol. Chem.* **267**:23226–23231.